

Nature of the magnetic order in superconducting and nonsuperconducting $\text{HoNi}_{2-x}\text{Co}_x\text{B}_2\text{C}$

J. W. Lynn and Q. Huang

*Reactor Radiation Division, National Institute of Standards and Technology, Gaithersburg, Maryland 20899
and University of Maryland, College Park, Maryland 20742*

A. Santoro

Reactor Radiation Division, National Institute of Standards and Technology, Gaithersburg, Maryland 20899

R. J. Cava, J. J. Krajewski, and W. F. Peck, Jr.

AT&T Bell Laboratories, Murray Hill, New Jersey 07974

(Received 4 May 1995; revised manuscript received 8 September 1995)

Neutron-diffraction measurements have been carried out to investigate the magnetic properties of superconducting ($T_c \sim 8$ K) $\text{HoNi}_2\text{B}_2\text{C}$ and nonsuperconducting ($T_c < 3$ K) $\text{HoNi}_{1.985}\text{Co}_{0.015}\text{B}_2\text{C}$. Both systems become magnetically long-range ordered below ~ 8 K, with three types of magnetic order being present. The low-temperature structure is a commensurate antiferromagnetic state that consists of Ho^{3+} moments aligned ferromagnetically in the a - b plane, with the sheets coupled antiferromagnetically along the c axis. The magnetic state that initially forms on cooling, however, is dominated by an incommensurate spiral antiferromagnetic state along the c axis, with wave vector $q_c \approx 0.054 \text{ \AA}^{-1}$, in which the relative alignment of each ferromagnetic sheet is rotated in the a - b plane by $\sim 17^\circ$ from the low-temperature antiparallel configuration. The intensity for this spiral state reaches a maximum near ~ 5 K; the spiral state then collapses at lower temperature in favor of the commensurate antiferromagnetic state. A smaller amplitude a -axis modulation, with $q_a \approx 0.73 \text{ \AA}^{-1}$, is also observed above the spiral antiferromagnetic transition, but over a narrower temperature range than the spiral state. The identical sequence of phase transitions is observed for both the superconducting and nonsuperconducting samples, demonstrating that the reentrant superconductivity and the coexistence of long-range antiferromagnetic order and superconductivity at low temperatures are both controlled by the nature of the magnetic structures present. In the temperature regime where the three magnetic structures are observed simultaneously, the sample dependence of the intensities strongly suggests that they occur in spatially separate regions.

I. INTRODUCTION

The discovery of superconductivity in $R\text{Ni}_2\text{B}_2\text{C}$ (R =rare earth element) and related materials has generated considerable interest in the superconductivity community for a number of reasons.¹⁻⁵ These are the first quaternary intermetallic systems that are superconducting, and they also appeared to be the first "high- T_c " [up to 23 K for $\text{YPd}_2\text{B}_2\text{C}$ (Ref. 2)] materials that do not contain either copper or oxygen. In these materials the planar Cu-O layers, which are thought to be essential to high- T_c superconductivity, are replaced by square-planar Ni layers. However, both measurements of the physical properties as well as band structure calculations⁶ show that these new materials are three dimensional in their behavior, and thus are in fact quite different than the layered cuprates. The substantial isotope effect⁷ and the nature of the electronic properties,⁸ as well as theoretical calculations, all show that the electron-phonon interaction is strong in these systems, and the high T_c is now thought to originate from a peak in the electronic density of states at the Fermi surface. In addition, the strong suppression of the superconducting transition temperature with magnetic doping onto the Ni lattice⁹ strongly indicates that these are conventional electron-phonon superconductors.

One of the truly unique characteristics of this new class of materials, on the other hand, is the high magnetic ordering temperatures of the heavy rare earth sublattice,¹⁰ with mag-

netic transition temperatures T_N as high as 20 K for $\text{GdNi}_2\text{B}_2\text{C}$.¹¹ The much higher magnetic transition temperatures ensure that the magnetic energetics for these new systems are dominated by exchange rather than dipolar (electromagnetic) interactions. The interplay between superconductivity and magnetism should therefore be much stronger than in the ternary Chevrel-phase and related systems,¹² where the magnetic ordering temperatures are typically ≤ 1 K, comparable to the expected dipolar ordering temperatures. This has indeed turned out to be the case, as exemplified by $\text{HoNi}_2\text{B}_2\text{C}$. This system becomes superconducting^{10,13} at $T_c \approx 8$ K while developing long-range magnetic order at about the same temperature.¹⁴ The temperature and field dependence of the magnetic order has been studied in some detail with neutrons,^{14,15} and complete profile refinements of both the nuclear and magnetic structures have also been carried out.¹⁶ Two types of magnetic order were initially observed, and are shown in Fig. 1. The commensurate antiferromagnetic structure consists of sheets of ferromagnetic moments in the a - b plane, with adjacent sheets coupled antiferromagnetically along the c axis [Fig. 1(a)]. The incommensurate spiral state is then obtained by rotating the direction of these ferromagnetic sheets in the a - b plane by an angle $\phi \sim 17^\circ$. The intensities from both types of Bragg peaks develop at about the same ordering temperature and initially grow with decreasing temperature at the same rate. At ~ 5 K the superconductivity is reentrant as evi-

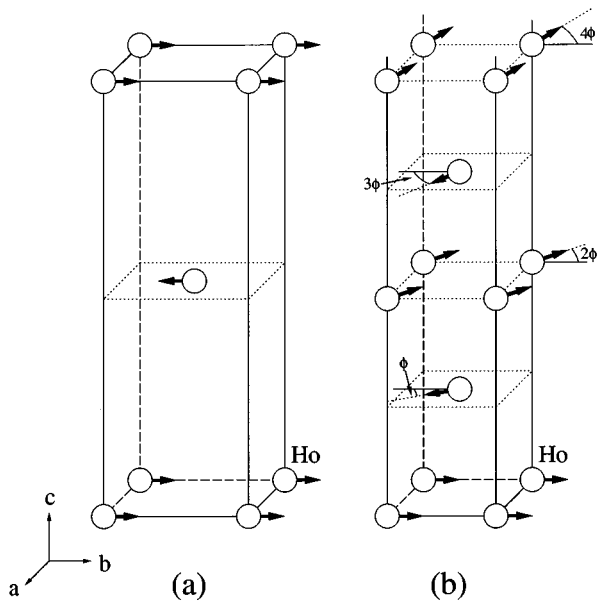


FIG. 1. Magnetic structures that have been determined for $\text{HoNi}_2\text{B}_2\text{C}$: (a) commensurate antiferromagnetic structure and (b) c -axis spiral. In each case the holmium moments are perpendicular to the c axis.

denced by a deep minimum in H_{c2} near 5 K,¹⁰ below which the incommensurate spiral order is suppressed in favor of a simple commensurate antiferromagnetic structure. This lock-in magnetic transition then permits the return of superconductivity and a coexistence of long-range antiferromagnetic order and superconductivity at low temperature.

In addition to the primary spiral and antiferromagnetic states just discussed, Goldman *et al.*^{17,18} also found incommensurate magnetic Bragg peaks along the a axis above 5 K, which corresponded to some kind of a short-wavelength modulated magnetic state that has a temperature dependence that was qualitatively, but not quantitatively, like the spiral state. The magnetic structure for these a -axis peaks has not been determined yet for $\text{HoNi}_2\text{B}_2\text{C}$, but they are similar to the peaks observed in $\text{ErNi}_2\text{B}_2\text{C}$,^{19,20} which is the only other magnetic superconductor in this class of materials that has been investigated so far with neutrons. The Er system becomes superconducting at $T_c \approx 11$ K and orders antiferromagnetically at $T_N = 6.8$ K. The magnetic order is described in terms of a relatively simple, incommensurate, transversely polarized spin-density-wave state along the a axis (or equivalently along the b axis in this tetragonal system). The modulation wave vector was found to be a temperature-independent value of $0.5526(2\pi/a)$, with the spin density wave squaring up at low temperatures. The magnetic order and superconductivity were found to coexist over the full temperature range where they are observed, with only a weak interaction between the two. It is likely that the magnetic structure associated with the a -axis peaks in $\text{HoNi}_2\text{B}_2\text{C}$ is a similar spin-density-wave configuration. However, since only the $\text{HoNi}_2\text{B}_2\text{C}$ system exhibits a giant anomaly in H_{c2} and reentrant superconductivity, and is also the only system that possesses the c -axis spiral, it seems clear that the magnetism associated with the a -axis peaks in

$\text{HoNi}_2\text{B}_2\text{C}$ is likely not controlling the reentrant superconducting behavior.

In our first experiments there were several questions that arose which required further investigation. For example, it was not clear whether the antiferromagnetic and spiral peaks represented a single, coherent magnetic structure, or whether they were different magnetic phases originating from different regions of the sample. This is also the case for the a -axis peaks. The purpose of the present study is then to investigate the sample dependence of these three types of magnetic peaks in order to ascertain whether they are separate magnetic phases or represent a single (or possibly two) coherent spin configurations. We also wanted to determine how each phase is related to the presence or absence of superconductivity, and for this we investigated these three phases in a sample doped with a small amount of Co, which suppresses the superconductivity.⁹ We found that in nominally identical samples the strengths of these three types of magnetic peaks can be quite different. Indeed in a recent study of the phase composition of this system, Schmidt, Weber, and Braun²¹ found that for small variations in the composition the material can be either a pure superconductor, can be fully reentrant, or can be nonsuperconducting. These phases correspond nicely with the types of magnetic order we observe in the present study.

II. EXPERIMENTAL PROCEDURES

Three polycrystalline samples were used in this study, and were prepared by the identical procedures used previously. The boron-11 isotope was used to reduce the nuclear absorption. The first sample (designated No. 1) is in fact the original 7 g sample we employed previously in our neutron studies.^{14–16} The second sample (No. 2) was made with the same nominal composition, but was found to be “more reentrant”; that is, the minimum in H_{c2} was deeper and wider in comparison to sample No. 1. The third sample was prepared with the composition $\text{HoNi}_{1.985}\text{Co}_{0.015}\text{B}_2\text{C}$, that is, 3/4% Co substitution on the Ni site, which is sufficient to reduce the superconducting transition temperature below 3 K.⁹ Indeed in this sample no superconductivity was detected for temperatures as low as 3 K. The latter two samples weighed 2 g each.

The temperature-dependent neutron-diffraction experiments were carried out on the HB-3 spectrometer at the High Flux Isotope Reactor at Oak Ridge National Laboratory. A pyrolytic graphite monochromator and filter were employed at a wavelength of 2.351 Å in the usual manner. The collimation before and after the sample was 20' full width at half maximum. An ILL-type top loading cryostat was used to cool the sample, and the sample temperature was controlled with a TRI controller. This configuration was employed to determine the magnetic order parameters as a function of temperature for each sample.

High-resolution powder-diffraction data were also obtained on the HB-4 powder diffractometer at a few selected temperatures. These data were then used to obtain complete structural refinements for the three samples, with the aim of correlating changes in the crystal structure with changes in the magnetic and superconducting phases. However, even though there were clear differences in the magnetic ordering

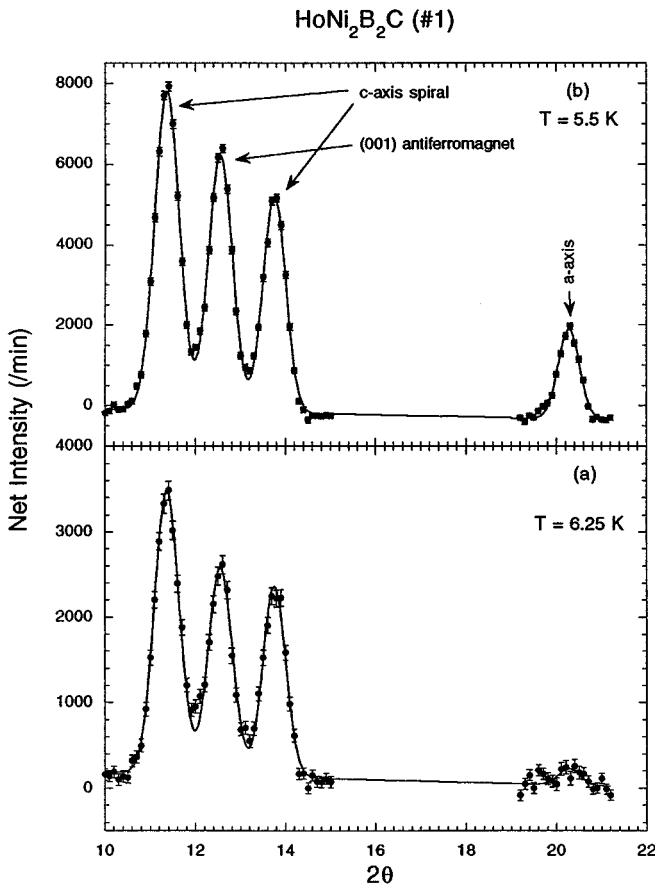


FIG. 2. Magnetic Bragg peaks observed for sample No. 1 of $\text{HoNi}_2\text{B}_2\text{C}$ at (a) 6.25 K and (b) 5.5 K. The three-peak structure consists of the commensurate antiferromagnetic peak in the center and the incommensurate c -axis spiral satellite peaks on either side. At 5.5 K the incommensurate a -axis peak is also evident.

in the samples, there were no systematic trends that could be identified in the refinements, within the experimental uncertainties typically obtained in these studies.¹⁶ Hence the variation in the composition that is producing these changes in the magnetic structures is subtle enough to be below these detection limits.

III. RESULTS

Figure 2(a) shows the scattering observed at a temperature of 6.25 K in the vicinity of the (001) antiferromagnetic peak position. The three-peak structure on the left replicates our original data on this sample, with the antiferromagnetic (001) peak in the center and the two incommensurate spiral satellite peaks on either side. The position of the spiral peaks has been found to be essentially temperature (and field) independent,^{14,15} and thus in the present study we simply monitored the peak intensities as a function of temperature as given below. The scattering on the right of the figure shows where the incommensurate a -axis magnetic peak is observed, and at this temperature there is very little intensity at this position. Indeed in order to obtain convergence at this temperature we had to fix the width to the instrumental width, and the position to the value found at lower T , in the

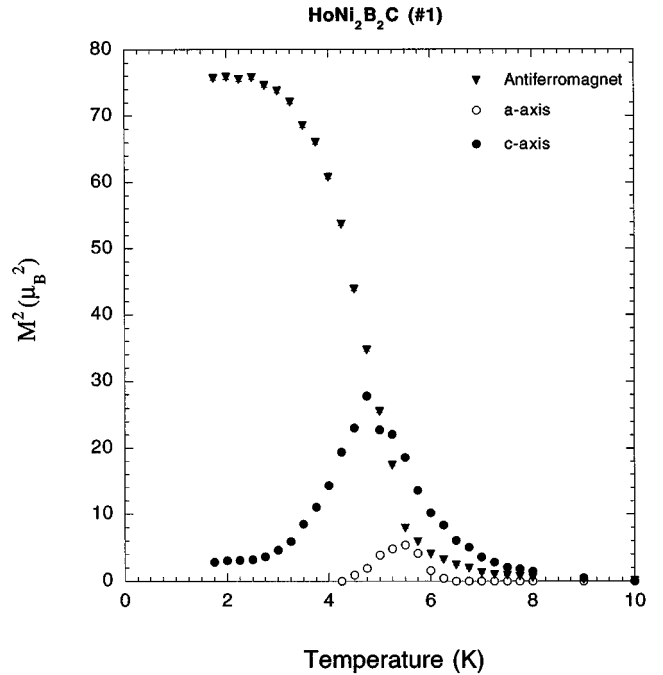


FIG. 3. Intensity for the commensurate antiferromagnetic Bragg peak (in μ_B^2) as a function of temperature, compared with the incommensurate c -axis spiral and a -axis intensities, for sample No. 1.

least squares fit. However, at a temperature of 5.5 K we observe a well-defined a -axis peak as shown in Fig. 2(b), and here there is no difficulty in fitting this peak. At still lower T this a -axis peak is again absent, and thus the intensity of this a -axis peak is strongly temperature dependent. We remark that all the a -axis data we present were obtained by measuring the full profile of the peak since we did not know if the position would be temperature dependent, but the position in fact turns out to be only very weakly temperature dependent. Finally we note that in addition to this a -axis peak the intensities of the spiral and antiferromagnetic peaks have approximately doubled in strength in comparison to the data at 6.25 K.

The temperature dependence of these three types of peaks is shown in Fig. 3. The data have been normalized with respect to the integrated magnetic scattering observed at low temperature, and the antiferromagnetic intensity is plotted as the square of the ordered moment. The magnetic structure for the c -axis spiral peaks is also known,^{14,16} and the observed satellite intensity at any given temperature can then be compared directly with the antiferromagnetic intensity. We remark that if the ordered moments for the spiral and antiferromagnetic structures were the same (and the fraction for each phase were identical), then the two satellite peaks in Fig. 2 *added together* would equal the intensity of the antiferromagnetic peak.²² Hence when the sample initially orders magnetically the ordered moment in the spiral phase is either $\sim\sqrt{2}$ larger than in the antiferromagnetic phase, or (more likely) the phase fraction that orders with the spiral structure is twice that for the antiferromagnetically ordered phase fraction. For this latter case the maximum value of the ordered moment in the spiral phase is then $\sim 6.7\mu_B$ when the spiral to antiferromagnetic lock-in transition is encountered, which

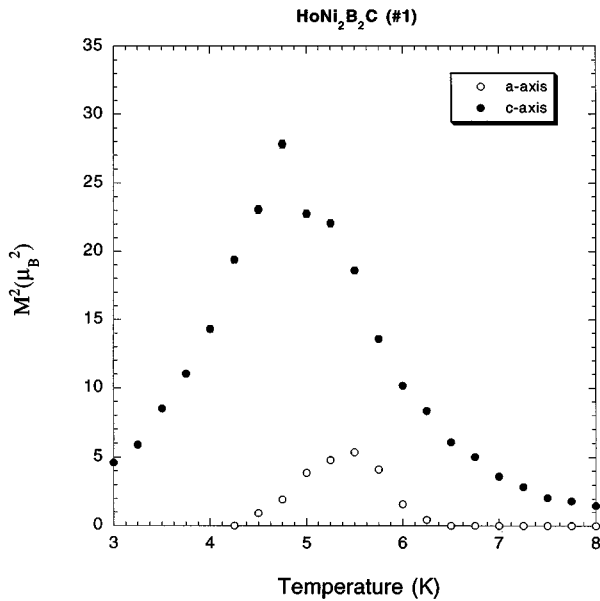


FIG. 4. Expanded view of the spiral and a -axis intensities, taken from Fig. 3.

is close to the full saturated value of $8.7\mu_B$ measured at low temperatures. For the a -axis peak, on the other hand, we have (arbitrarily) scaled its intensity with respect to the c -axis spiral in order to maintain the same relative intensities between these two, since the magnetic structure for the a -axis-type peaks is not yet known. The statistical error bars have also been plotted in Fig. 3 but are typically smaller than the data points. In our previous studies we found that there is substantial hysteresis as a function of temperature (and magnetic field), and thus the data shown here and those given below were all obtained on the cooling cycle so that they may be readily compared.

Figure 4 shows the intensity of the spiral and a -axis peaks on an expanded scale. It can be noticed that there is some observable intensity at the spiral position even at 9 K, while at 8 K a well-defined three-peak structure has already developed.¹⁵ In order to observe a well-defined three-peak structure in a powder, with resolution-limited peak widths, we must either have a very long correlation length ($\xi > 500$ Å), or a true long-range-ordered state. The first case would indicate that we are very near the ordering temperature, and long-range order would then set in just below ~ 8 K. We are therefore led to the conclusion that the magnetic ordering temperature is very close to 8 K (and thus close to T_c). We note that the intensity of the spiral peak grows in a continuous fashion, but with a concave-upward curvature. This shape has been found for all the samples studied to date, both powders and single crystals. In view of the strong dependence of the magnetic properties on subtle composition changes, we believe that this behavior is most likely the result of having a distribution of transition temperatures. We point out, however, that this shape could also result if the magnetic interactions were highly anisotropic, such as for low-dimensional systems.²³ In these Ni systems, though, there is no evidence for low-dimensional behavior, and we discard this possibility. Another possibility is if the critical exponent $\beta > \frac{1}{2}$, with $I \propto (T_N - T)^{2\beta}$, where the intrinsic in-

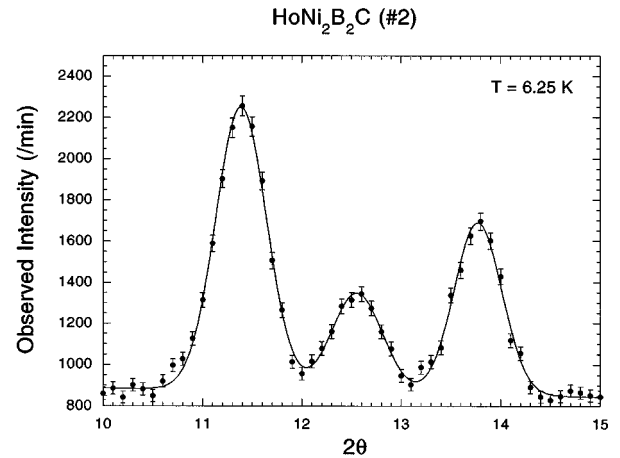


FIG. 5. Antiferromagnetic and c -axis spiral Bragg peaks at 6.25 K for sample No. 2. Note that the relative intensity of the antiferromagnetic peak is reduced by a factor of 2.3 with respect to the spiral peaks for this sample in comparison to sample No. 1 (Fig. 2), indicating that these peaks originate from separate regions of the sample.

tensity is concave upward. Finally, we note that this type of behavior is observed in the case when no phase boundary is crossed.²⁴ Clearly the magnetic critical scattering (if it exists) in these systems would be interesting to investigate when samples of sufficient uniformity become available.

We noted previously that the spiral and antiferromagnetic peaks initially grow at the same rate with decreasing temperature, but then the rate of growth of the spiral peak slows and the intensity has a maximum at ~ 5 K, close to the reentrant superconducting transition temperature. The intensity then drops rapidly as the antiferromagnetic peak increases rapidly. The a -axis peak, on the other hand, has no observable intensity above ~ 6.5 K, maximizes at 5.5 K, and then becomes unobservable below 4.5 K. The temperature dependence for the a -axis and c -axis peaks is thus quite different, suggesting that these peaks originate from different regions of the sample. Note in particular that the temperatures at which the maxima occur are clearly quite different in this sample. Goldman *et al.*,¹⁷ on the other hand, found that the maxima occurred at approximately the same temperature. This difference in the temperature dependence for different samples also suggests that these two peaks belong to separate magnetic phases.

The three-peak structure for the second sample of $\text{HoNi}_2\text{B}_2\text{C}$ is shown in Fig. 5 at a temperature of 6.25 K. In comparison with the first sample, we note that the intensity of the antiferromagnetic peak is about 2.3 times smaller compared to the spiral peaks than in the first sample, even though the antiferromagnetic and spiral orderings again occur at about the same ordering temperature. Thus the ratio of intensities is again approximately independent of temperature (until the spiral intensity gets close to the maximum), and we conclude that the spiral and antiferromagnetic intensities originate from separate magnetic phases in the sample.

The temperature dependence of the magnetic intensities is shown in Fig. 6. We see that the overall behavior is quite similar for the two samples, but in detail they are different as shown in the expanded view given in Fig. 7. We see that the

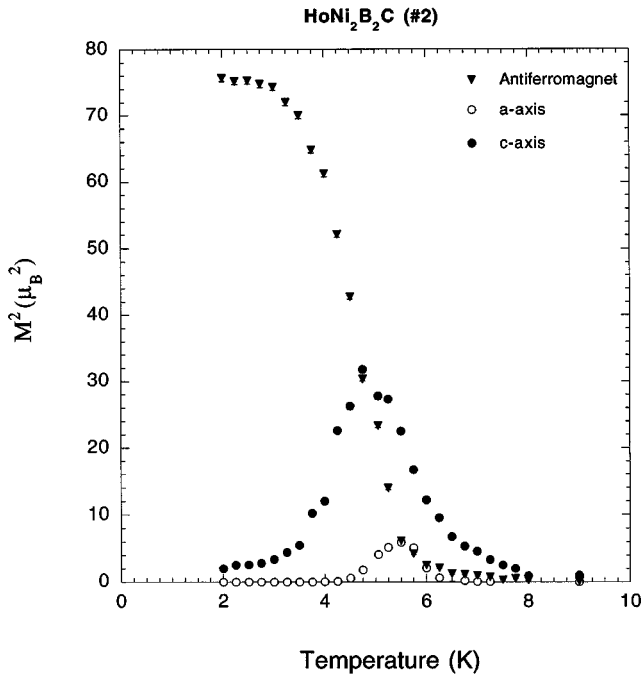


FIG. 6. Intensity for the commensurate antiferromagnetic Bragg peak (in μ_B^2) as a function of temperature, compared with the incommensurate c -axis spiral and a -axis intensities, for sample No. 2.

amplitude of the spiral peak is somewhat larger than for sample No. 1, which we believe correlates with the deeper and wider reentrant feature observed in the susceptibility measurements. The a -axis feature, on the other hand, is very similar for the two samples. Thus it is again clear that the spiral feature is associated with the reentrant superconducting behavior.

Finally, we took data on the Co-doped sample, which is not superconducting above 3 K. The overall behavior for the

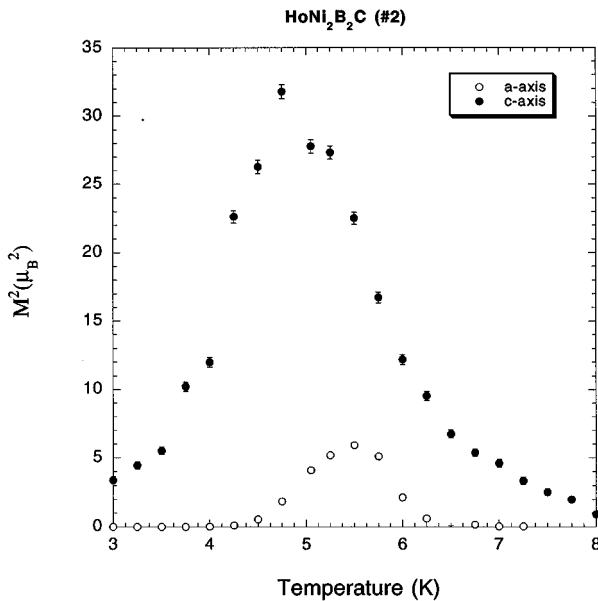


FIG. 7. Expanded view of the spiral and a -axis intensities, taken from Fig. 6.

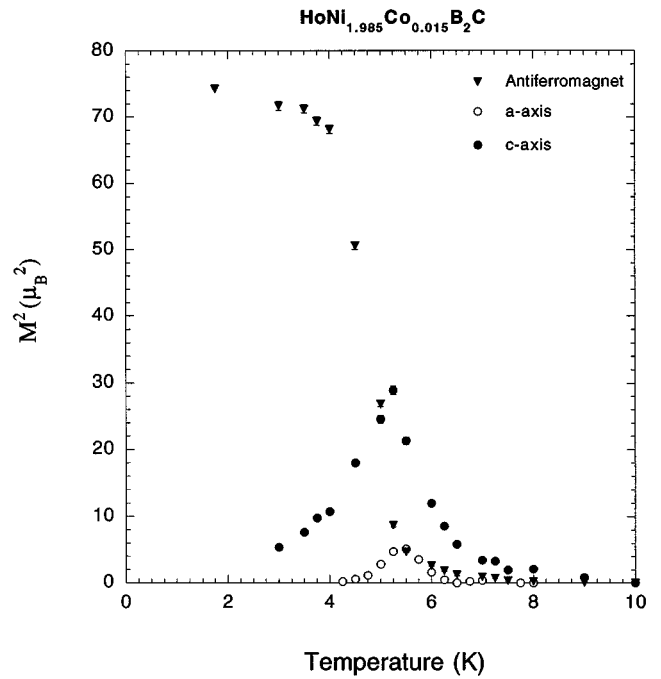


FIG. 8. Intensity for the commensurate antiferromagnetic Bragg peak (in μ_B^2) as a function of temperature, compared with the incommensurate c -axis spiral and a -axis intensities, for the nonsuperconducting ($T_c < 3$ K) composition $\text{HoNi}_{1.985}\text{Co}_{0.015}\text{B}_2\text{C}$.

antiferromagnetic, spiral, and a -axis phases is quite similar to that shown for the previous two reentrant-superconducting samples, as shown in Fig. 8. The expanded view is shown in Fig. 9, where we have also plotted the data for sample No. 2 (Fig. 4) for comparison. We see that the maximum scattering strength for the spiral and a -axis peaks is about the same as

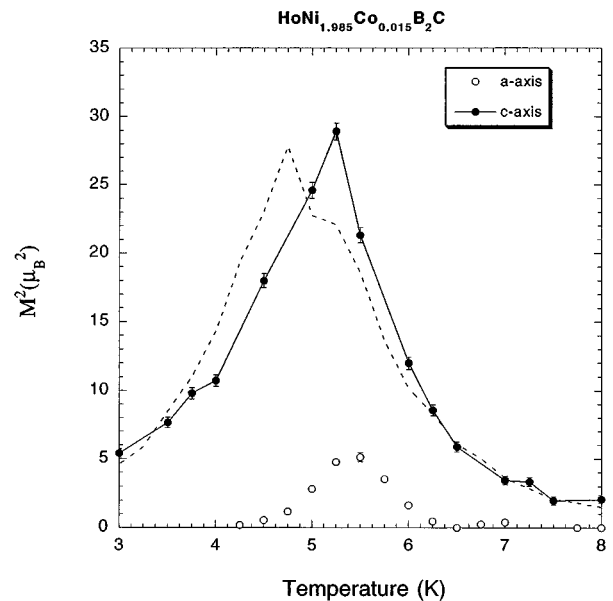


FIG. 9. Expanded view of the spiral and a -axis intensities, taken from Fig. 8. The dashed curve is the data for the superconducting sample, taken from Fig. 4, for comparison purposes, while the solid curve just connects the c -axis data points.

for the superconducting samples. The maxima for the a -axis and c -axis peaks again occur at different temperatures for the Co-doped sample, although they are not as far apart in T as for the other two samples. Our conclusion is that the antiferromagnetic, c -axis spiral, and a -axis orderings are separate phases that develop as a function of temperature, and they are to a good approximation independent of whether or not the system is superconducting. The superconductivity, then, will only be present in the system if the nature of the magnetic ordering allows such a coexistence.

IV. DISCUSSION

There are three types of magnetic peaks in the $\text{HoNi}_2\text{B}_2\text{C}$ system, the commensurate antiferromagnet, a c -axis spiral phase, and the a -axis peaks. The antiferromagnet and spiral phases are the dominant ones in these samples with nominal composition $\text{HoNi}_2\text{B}_2\text{C}$. The data show that these two components develop at about the same temperature for all the samples studied, but belong to different phases, with the phase fraction exhibiting a strong variation between samples. At low T the antiferromagnet is the only phase that is present,¹⁵ and this phase is known to readily coexist with superconductivity. Hence if in a particular region of the sample this is the phase that initially forms on cooling, then we expect little interaction with the superconductivity over the entire temperature range. In the compositional study of Schmidt, Weber, and Braun,²¹ they find a superconducting phase that exhibits no reentrance, and we believe that this is the material that initially orders as a commensurate antiferromagnet.

If a region of the sample initially orders in the c -axis spiral state, on the other hand, then we expect to have a strong interaction with the superconductivity because there is a net uncompensated ferromagnetic component on the Ni layer from the adjacent Ho layers.¹⁴ As the amplitude of the spiral state grows, the superconductivity is extinguished. The ordered moment in the spiral state becomes quite large ($\sim 6.7\mu_B$), but then a magnetic lock-in transition to the commensurate antiferromagnetic state occurs which allows the superconductivity to return and coexist. Since we observe the same sequence of phase transitions whether or not the material is superconducting, it is clear that the magnetism is controlling whether the superconductivity is present or not. In particular, we believe that the magnetic lock-in transition is controlled by the magnetic properties alone, with little influ-

ence caused by the superconductivity when it is present. This complete dominance of the magnetism is different from the well-known ferromagnetic-superconductor systems such as HoMo_6Se_8 (Ref. 25) and ErRh_4B_4 ,^{26,27} where the coupling between the ferromagnetism and superconductivity (with $T_M < T_c$) initially forces the appearance of an oscillatory magnetic state just below the magnetic ordering temperature T_M . Even in these materials, though, the magnetism wins at sufficiently low T and there is a lock-in transition to a pure ferromagnetic state which extinguishes the superconducting state. For HoMo_6Se_8 ,²⁸ on the other hand, the magnetic moment is smaller while the T_c is larger than for HoMo_6Se_8 , we find a strong temperature dependence to the spiral wave vector while the superconductivity survives at low T . $\text{HoNi}_2\text{B}_2\text{C}$ appears to be in the opposite situation where the moment and the magnetic ordering temperature are large, and thus the magnetism dominates at all temperatures.

The a -axis peaks have a temperature dependence that is clearly quite different than the spiral phase, and this argues that the c -axis and a -axis peaks also belong to separate magnetic phases. However, there is no dramatic variation in their relative intensities from sample to sample, and therefore we feel that the conclusion that they belong to separate phases is a less compelling conclusion than for the antiferromagnetic and spiral phases. It is also not clear what the relationship is between the a -axis peaks and the presence or absence of superconductivity. Unfortunately, the relatively weak scattering from these peaks has so far precluded us from solving the magnetic structure via powder profile refinement, while extinction and other experimental difficulties have so far prohibited the solution of any of these magnetic (or chemical) structures via single-crystal diffraction.¹⁷ Finally, we note that these incommensurate magnetic phases are very sensitive functions of the composition and/or state of the sample, and the property that is controlling the appearance of these various magnetic phases has not been identified yet.

ACKNOWLEDGMENTS

We would like to thank Bryan Chakoumakos, Jaime Fernandez-Baca, and Brent Taylor for their generous assistance while we were visiting Oak Ridge National Laboratory. We would also like to thank H. Schmidt, M. Weber, and H. F. Braun for communicating their results prior to publication. Research at the University of Maryland is supported in part by the NSF Grant No. DMR 93-02380.

¹R. Nagarajan, C. Mazumdar, Z. Hossain, S. K. Dhar, K. V. Gopalakrishnan, L. C. Gupta, C. Godart, B. D. Padalia, and R. Vijayaraghavan, *Phys. Rev. Lett.* **72**, 274 (1994).

²R. J. Cava, H. Takagi, B. Batlogg, H. W. Zandbergen, J. J. Krajewski, W. F. Peck, Jr., R. B. van Dover, R. J. Felder, T. Siegrist, K. Mizuhahi, J. O. Lee, H. Eisaki, S. A. Carter, and S. Uchida, *Nature* **367**, 146 (1994).

³R. J. Cava, H. Takagi, H. W. Zandbergen, J. J. Krajewski, W. F. Peck, Jr., T. Siegrist, B. Batlogg, R. B. van Dover, R. J. Felder, K. Mizuhashi, J. O. Lee, H. Eisaki, and S. Uchida, *Nature* **367**, 252 (1994).

⁴T. Siegrist, H. W. Zandbergen, R. J. Cava, J. Krajewski, and W. F. Peck, Jr., *Nature* **367**, 254 (1994).

⁵R. J. Cava, H. W. Zandbergen, B. Batlogg, H. Eisaki, H. Tagaki, J. J. Krajewski, W. F. Peck, Jr., E. M. Gyorgy, and S. Uchida, *Nature* **372**, 759 (1994).

⁶L. F. Mattheiss, *Phys. Rev. B* **49**, 13 279 (1994); W. E. Pickett and D. J. Singh, *Phys. Rev. Lett.* **72**, 3702 (1994); L. F. Mattheiss, T. Siegrist, and R. J. Cava, *Solid State Commun.* **91**, 587 (1994); R. Coehoorn, *Physica C* **228**, 331 (1994); L. F. Mattheiss, *Phys. Rev. B* **47**, 8224 (1993).

⁷D. D. Lawrie and J. P. Franck (unpublished).

- ⁸S. A. Carter, B. Batlogg, R. J. Cava, J. J. Krajewski, W. F. Peck, Jr., and H. Tagaki, *Phys. Rev. B* **50**, 4216 (1994).
- ⁹H. Schmidt and H. F. Braun, *Physica C* **235-240**, 779 (1994).
- ¹⁰H. Eisaki, H. Takagi, R. J. Cava, K. Mizuhashi, J. O. Lee, B. Batlogg, J. J. Krajewski, W. F. Peck, Jr., and S. Uchida, *Phys. Rev. B* **50**, 647 (1994).
- ¹¹L. C. Gupta, R. Nagarajan, Z. Hossain, C. Mazumdar, S. K. Dhar, C. Godart, C. Levy-Clement, B. D. Padalia, and R. Vijayaraghavan, *J. Magn. Magn. Mater.* **140-144**, 2053 (1995); M. El Masalami and E. M. Baggio-Saitovitch (unpublished).
- ¹²For a thorough review of many aspects of magnetic superconductors, see *Topics in Current Physics*, edited by Ø. Fischer and M. B. Maple (Springer-Verlag, New York, 1983), Vols. 32 and 34.
- ¹³See also P. C. Canfield, B. K. Cho, D. C. Johnston, D. K. Finnemore, and M. F. Hundley, *Physica C* **230**, 397 (1994); P. C. Canfield, B. K. Cho, D. C. Johnston, and M. F. Hundley (unpublished).
- ¹⁴T. E. Grigereit, J. W. Lynn, Q. Huang, A. Santoro, R. J. Cava, J. J. Krajewski, and W. F. Peck, Jr., *Phys. Rev. Lett.* **73**, 2756 (1994).
- ¹⁵T. E. Grigereit, J. W. Lynn, R. J. Cava, J. J. Krajewski, and W. F. Peck, Jr., *Physica C* **248**, 382 (1995).
- ¹⁶Q. Huang, A. Santoro, T. E. Grigereit, J. W. Lynn, R. J. Cava, J. J. Krajewski, and W. F. Peck, Jr., *Phys. Rev. B* **51**, 3701 (1995); (unpublished).
- ¹⁷A. I. Goldman, C. Stassis, P. C. Canfield, J. Zarestky, P. Dervenagas, B. K. Cho, D. C. Johnston, and B. Sternlieb, *Phys. Rev. B* **50**, R9668 (1994); C. Stassis, A. I. Goldman, P. Dervenagas, J. Zarestky, P. C. Canfield, B. K. Cho, D. C. Johnston, and B. Sternlieb, *J. Mater. Res. Soc.* (to be published).
- ¹⁸See also C. V. Tomy, L. J. Chang, D. McK. Paul, N. H. Anderson, and M. Yethiraj, *Physica B* **213-214**, 139 (1995).
- ¹⁹S. K. Sinha, J. W. Lynn, T. E. Grigereit, Z. Hossain, L. C. Gupta, R. Nagarajan, and C. Godart, *Phys. Rev. B* **51**, 681 (1995).
- ²⁰J. Zarestky, C. Stassis, A. I. Goldman, P. C. Canfield, P. Dervenagas, B. K. Cho, and D. C. Johnston, *Phys. Rev. B* **51**, 678 (1995).
- ²¹H. Schmidt, M. Weber, and H. F. Braun, *Physica C* **235-240**, 779 (1994).
- ²²G. E. Bacon, *Neutron Diffraction* (Clarendon, Oxford, 1975), p. 269.
- ²³See, for example, J. W. Lynn, *J. Alloys Compounds* **181**, 419 (1992).
- ²⁴See, for example, J. M. Hastings, L. M. Corliss, W. Kummann, R. Thomas, R. J. Begum, and P. Bak, *Phys. Rev. B* **22**, 1327 (1980).
- ²⁵J. W. Lynn, G. Shirane, W. Thomlinson, and R. N. Shelton, *Phys. Rev. Lett.* **46**, 368 (1981); J. W. Lynn, A. Raggazoni, R. Pynn, and J. Joffrin, *J. Phys. (Paris) Lett.* **42**, L45 (1981).
- ²⁶D. E. Moncton, D. B. McWhan, P. H. Schmidt, G. Shirane, W. Thomlinson, M. B. Maple, H. B. MacKay, L. D. Woolf, Z. Fisk, and D. C. Johnston, *Phys. Rev. Lett.* **45**, 2060 (1980).
- ²⁷S. K. Sinha, G. W. Crabtree, D. G. Hinks, and H. A. Mook, *Phys. Rev. Lett.* **48**, 950 (1982).
- ²⁸J. W. Lynn, J. A. Gotaas, R. W. Erwin, R. A. Ferrell, J. K. Bhattacharjee, R. N. Shelton, and P. Klavins, *Phys. Rev. Lett.* **52**, 133 (1984).